Radical Shuttling in a Protein: Ribose Pseudorotation Controls Alkyl-Radical Transfer in the Coenzyme B$_{12}$ Dependent Enzyme Glutamate Mutase**

Karl Gruber,* Riikka Reitzer, and Christoph Kratky

Enzymatic reactions involving organic-radical intermediates are relatively rare, and occur when alternative (heterolytic) pathways would lead across prohibitively high activation barriers, for example, reactions at unactivated carbon centers.[1] Because of their substantial and unspecific reactivity, organic-radical intermediates have to be scrupulously controlled by the enzyme to prevent side reactions that may result in enzyme inactivation or damage, unwanted products, or the release of toxic radicals. Once a radical is generated, the major problem for the enzyme is to guide the "hot" intermediate along the desired reaction path, and not the enhancement the rate of subsequent steps. This constitutes Rétey's concept of "negative catalysis".[2]

In coenzyme B$_{12}$ dependent enzymes[3] (Scheme 1a) a catalytically relevant 5′-desoxyadenosyl (Ado) radical has long been known to be one of the products of substrate-induced homolytic cleavage of the cobalt–carbon bond of the cofactor.[4] This class of enzymes can therefore be regarded as a prime example of enzymatic utilization of an organic radical.

The Ado radical, formed by homolytic cleavage of the Co–C bond, abstracts a hydrogen atom from the substrate in the next reaction step. While this hydrogen abstraction involves, in some cases, the intermediate formation of a protein-bound thiyl radical (e.g. in ribonucleotide reductases),[5] direct interaction between the Ado radical and the substrate has been implicated for the majority of coenzyme B$_{12}$ dependent enzymes. Whereas the first steps are conceptually similar in all coenzyme B$_{12}$ dependent enzymes, the subsequent transformation of the substrate-derived radical to yield a product-related radical differs, although there are some mechanistic similarities.[6]

A long-standing question concerns the way in which the enzyme couples cleavage of the cobalt–carbon bond with substrate binding. In the case of methylmalonyl-CoA mutase[7, 8] this coupling has been attributed to a crystallographically detected substrate-induced conformational change. Equally important for the catalytic mechanism is the safe transfer of the "hot" C$_{5'}$-methylene radical from the cobalt to the substrate (Scheme 2). Structural[7, 9, 10] and EPR spectroscopy data[11–13] indicate that the reaction partner for this radical is 6–8 Å away from the cobalt center and kinetic data further suggest that the Ado radical is only present as an extremely short-lived intermediate.[14, 15]

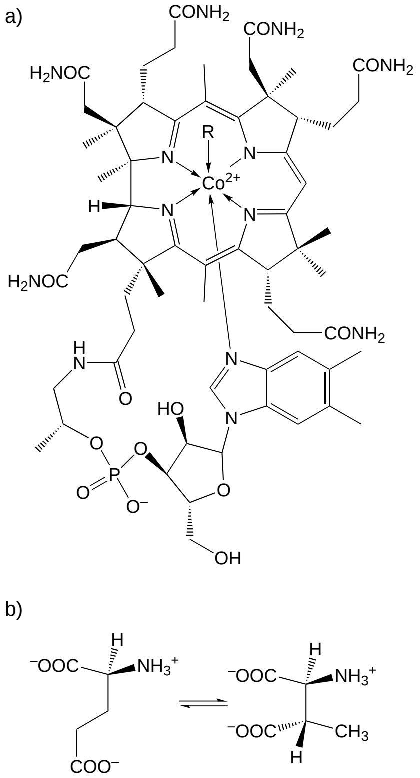

Scheme 1. a) Structural formula of some B$_{12}$ derivatives: 5′-desoxyadenosylcobalamin (coenzyme B$_{12}$, R = 5′-desoxyadenosyl$^-$), methylcobalamin (R = CH_3^-), cyanocobalamin (vitamin B$_{12}$, R = CN^-), and cob(II)alamin (B$_{12r}$, R = e$^-$). Note that the structural formula given correspond to the cofactor in solution. Upon binding to glutamate mutase, the dimethylbenzimidazole base is replaced by a protein-derived imidazole ring. b) Reaction catalyzed by glutamate mutase.

The coenzyme B$_{12}$ dependent glutamate mutase (Glm) catalyzes the interconversion of (*S*)-glutamate to (2*S*,3*S*)-3-methylaspartate (Scheme 1b). We recently determined the three-dimensional structure of the enzyme from *Clostridium cochlearium* by using inactive enzyme reconstituted with cyanocobalamin (vitamin B$_{12}$) and methylcobalamin[9] (Scheme 1a). Here, we report the crystal structure analysis at 1.9 Å resolution of active Glm with 5′-desoxyadenosylcobalamin (coenzyme B$_{12}$, Scheme 1) as cofactor in the presence of the substrate glutamate.

Residual electron density is clearly observed above the "upper" β-face of the corrin ring (Figure 1a) and can be attributed to the adenosyl group. However, to model the ribose portion of this density, a superposition of two species has to be invoked: species A with the ribose in a C$_{2'}$-*endo* and species B in a C$_{3'}$-*endo* conformation. In addition, the two conformers are shifted slightly with respect to each other and have an approximately 25° difference in the torsion angle about the glycosidic bond, which leads to a distance of 1.7 Å between the 5′-carbon atoms of the two conformers. In the

---

[*] Dr. K. Gruber, Dr. R. Reitzer, Dr. C. Kratky
Institut für Chemie
Universität Graz
Heinrichstrasse 28, 8010 Graz (Austria)
Fax: (+43) 316-380-9850
E-mail: karl.gruber@uni-graz.at

[**] This work was supported by the Österreichische Akademie der Wissenschaften (APART fellowship 614), the Österreichische Fonds zur Förderung der wissenschaftlichen Forschung (FWF-project 11599), and the European Commission (TMR project number ERB 4061 PL 95-0307). Crystallographic data were collected at the EMBL-beamline BW7B at DESY in Hamburg, Germany. We thank the beamline scientists for their assistance, and Ingrid Dreveny, Günter Gartler, Gerwald Jogl, and Oliver Sauer for their help during data collection. This research emerged from a collaboration with Prof. W. Buckel (Marburg) who supplied us with clones of the glutamate mutase proteins.

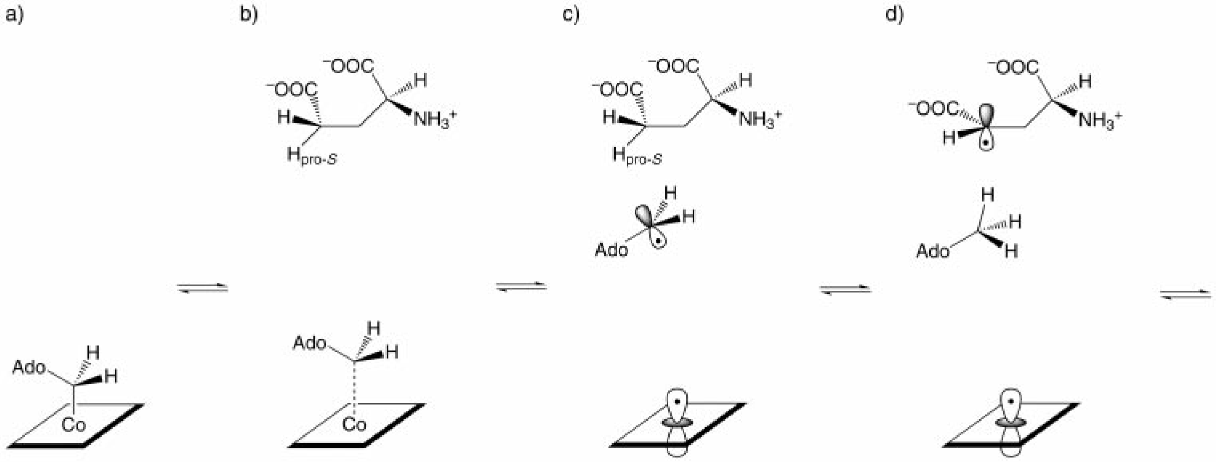

Scheme 2. The first steps along the reaction sequence catalyzed by glutamate mutase: a) the B_{12} cofactor without substrate; b) substrate binding induces Co–C homolysis through steric strain; c) following homolysis, the 5′-end of the Ado radical is transferred to the substrate; d) abstraction of a hydrogen atom from the substrate by the Ado radical leads to the formation of a 4-glutamyl radical and a protein-associated 5′-desoxyadenosine molecule.

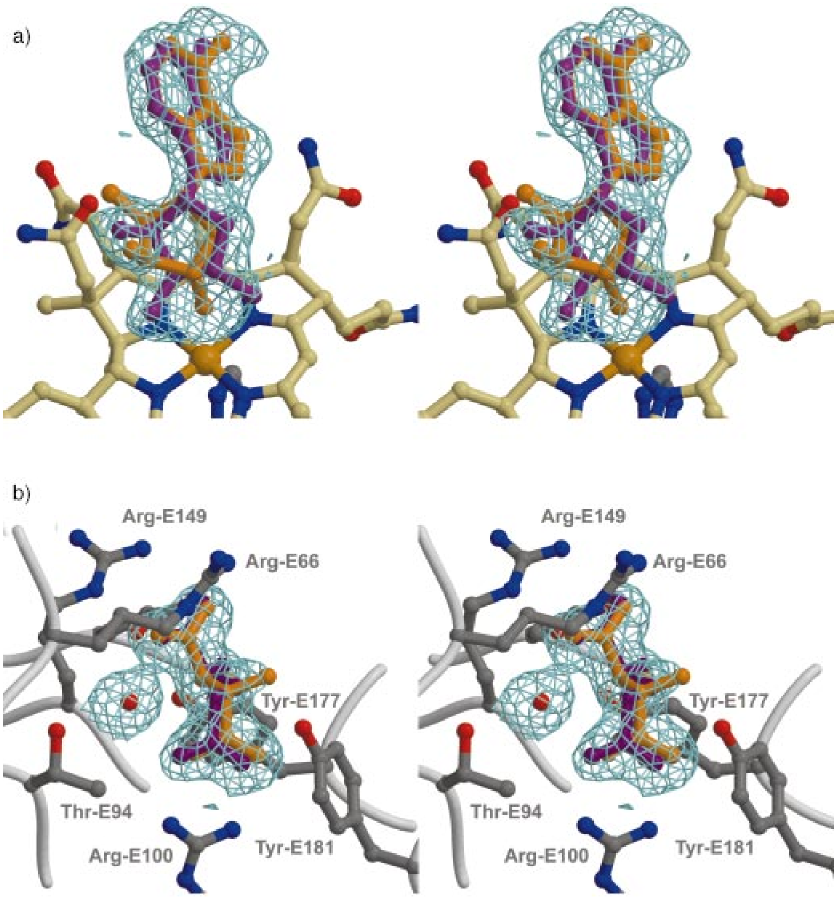

Figure 1. a) Difference electron density for the Ado ligand with the refined model of conformer A represented in orange, and conformer B in magenta. The mean *B* value for the ligand of 12 Å^2 is comparable to the 8 Å^2 observed for the surrounding protein and solvent atoms (within a maximum distance of 6 Å). The largest positional differences between the two conformers are observed for $O_{2'}$ (1.7 Å), $O_{3'}$ (2.9 Å), $C_{3'}$ (1.3 Å), and $C_{5'}$ (1.7 Å). The differences for the remaining atoms of the Ado group are around 0.6 Å or less. b) Difference electron density in the substrate binding site with glutamate shown in magenta and methylaspartate in orange. The relative occupancies after refinement were 30 % for glutamate and 70 % for methylaspartate with a mean *B* value of 7 Å^2. The density in (a) and (b) was calculated after the initial refinement without the Ado ligand and the substrate. Figure 1 and 2 were generated with the programs Molscript[23] and Raster3D.[24]

crystal investigated, conformations A and B occur in a 40:60 ratio, but different relative occupancies were found in other crystal specimens. Although the enzyme was crystallized in the presence of glutamate, the experimental density clearly shows that most of the glutamate has been converted into methylaspartate (Figure 1 b).

The distance between the 5′-carbon atom and the cobalt atom differs dramatically between the two conformers (3.1 – 3.2 Å for A and about 4.5 Å for B). While $C_{5'}$ is positioned above the metal center in A (Figure 2 a), it is displaced towards the substrate binding site in B (Figure 2 b), where it is within van der Waals distance from the substrate and would thus be ideally positioned for hydrogen atom exchange with the substrate.

The interaction between the Ado group and the protein is very similar for the two conformers and involves hydrogen bonds from the adenine to main-chain carbonyl atoms, to the c-acetamide side chain of the cofactor, and to two water molecules (Figure 2). The ribose hydroxyl groups form hydrogen bonds to Glu 330, Lys 326, and one water molecule. The latter hydrogen-bonding pattern differs somewhat between the two conformers (Figure 2).

The two crystallographically observed Ado species can be interpreted to correspond to intermediates along the Glm-catalyzed reaction path. If this interpretation is correct, species A is an activated cofactor molecule with a highly strained (3.2 Å long) Co–C bond (Scheme 2 b) and species B is a 5′-desoxyadenosine resulting from H-atom abstraction by the Ado radical from the substrate (Scheme 2 c).[16]

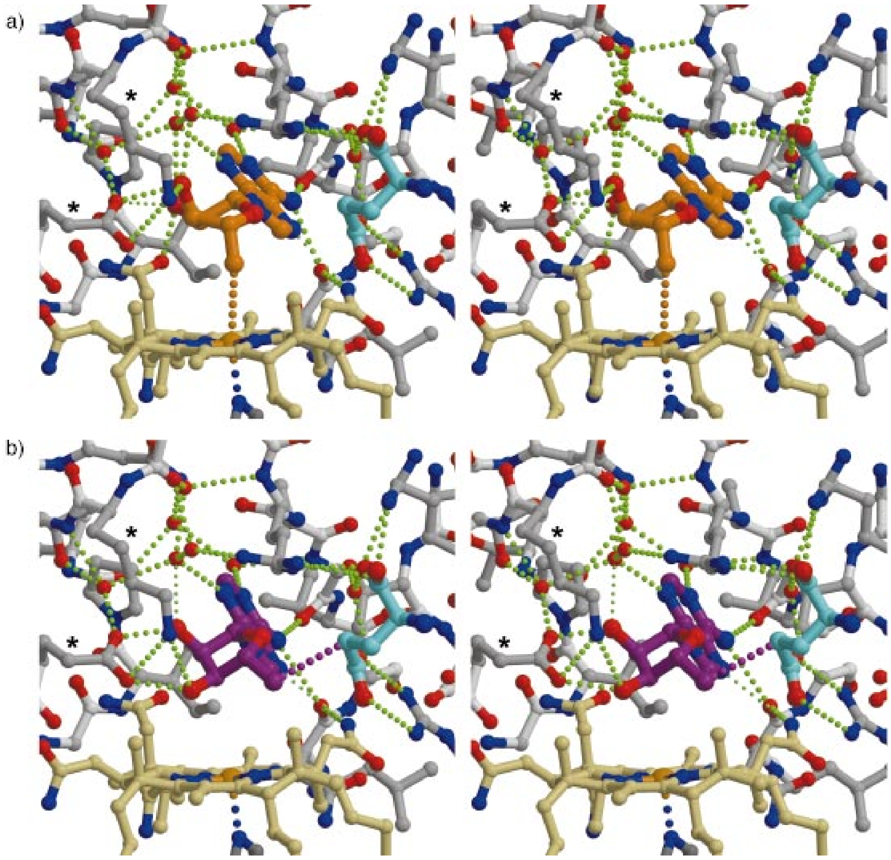

Figure 2. Stereoscopic views of the cofactor and substrate binding site and the interactions of conformers A (a) and B (b) of the adenosyl ligand. The coloring scheme for carbon atoms is as follows: protein main chain: white; side chain: light gray; Ado group: orange and magenta; corrin ring: yellow; substrate (glutamate): cyan. Nitrogen and oxygen atoms are colored blue and red, respectively. Lines of small green spheres denote hydrogen bonding interactions, lines of orange and magenta spheres indicate interactions of the ribose-$C_{5'}$ with the cofactor (a) and the substrate (b), respectively, lines of small blue spheres indicate the interaction of the cobalt atom with the imidazole of His16. Residues Glu330 and Lys326 are marked with asterisks.

These two observed species suggest how glutamate mutase affords a safe and energetically facile transport of the $C_{5'}$-radical atom from the cobalt center to the substrate: Ribose pseudorotation between the two minimum-energy conformations $C_{2'}$-*endo* and $C_{3'}$-*endo* involves a very low energy barrier,[17] yet it rigidly constrains the trajectory of the $C_{5'}$-atom with well defined endpoints. The overall position and orientation of the ribose ring is restrained by hydrogen bonds to the side chains of residues Glu330 and Lys326 (Figure 2). We believe that this discovery constitutes a perfect example for the concept of "negative catalysis": enzymes have to exert tight control on high-energy intermediates to prevent them from entering into deactivating side reactions.[2]

The radical-shuttling mechanism proposed here almost certainly also applies to the coenzyme B_{12} dependent methylmalonyl-CoA mutase, for which the concept of "negative catalysis"[2] was originally suggested. The structure of the active site (including the conserved glutamate) and the relative arrangement of cofactor and substrate[7, 18] are strikingly similar to those of Glm. It remains to be seen which other coenzyme B_{12} dependent enzymes have solved the radical-transfer problem in a similar fashion.[19]

Experimental Section

Recombinant glutamate mutase from *Clostridium cochlearium* was overproduced, reconstituted with 5′-desoxyadenosylcobalamin, and purified as described previously.[9] Crystals of up to $0.2 \times 0.2 \times 0.05$ mm were obtained by using the sitting-drop method. Drops of 4 µL containing protein (3.5 mg mL^{-1}), coenzyme B_{12} (0.5 mg mL^{-1}), and $CdCl_2$ (2 mM) were mixed with reservoir solution (4 µL containing 6% (w/v) PEG-4000 in 0.1M Na-*S*-glutamate, pH 4.5) and equilibriated. Purification and crystallization were performed under red light to prevent photolytic degradation of the cofactor. This precaution was somewhat relaxed once the crystals were frozen.

Diffraction data were collected from a flash-cooled crystal (cryoprotected with 30% glycerol) at EMBL-beamline BW7B ($\lambda = 0.8439$ Å) at DESY in Hamburg, Germany, and were processed and scaled using DENZO and SCALEPACK.[20] A starting model was obtained by using the coordinates of the cyanocobalamin reconstituted glutamate mutase (PDB-entry 1CCW)[9] after removal of solvent, cofactor, and substrate atoms. After rigid-body refinement strong residual density was observed for the cofactor (including the Ado ligand) as well as the substrate. The completed model was refined with SHELXL-97[21] as described previously.[9] Details of the structure determination are listed in Table 1. Coordinates have been deposited with the Protein Data Bank with accession code 1I9C.

Received: January 25, 2001
Revised: June 22, 2001 [Z16510]

Table 1. Data collection and refinement statistics.

space group	$P2_1$
unit cell dimensions	$a = 64.3$ Å $b = 113.1$ Å $c = 108.4$ Å $\beta = 96.0°$
temperature	−170 °C
resolution	30–1.9 Å
observed reflections[a]	555148 (30037)
unique reflections[a]	121680 (8102)
completeness[a] (theoretically possible reflections actually collected)	99.9% (100%)
mean $I/\sigma(I)$[a]	18.4 (5.0)
R_{sym}[a]	0.073 (0.281)
$I > 2\sigma(I)$[a]	92.1% (91.4%)
number of protein atoms	9738
number of solvent molecules (H_2O)	1258
number of B_{12} cofactor and substrate atoms	294
R_{cryst}[b]	0.168 (0.157)
R_{free}[b,c]	0.221 (0.201)
average *B* values	
protein	12 Å^2
solvent	24 Å^2
B_{12} cofactor, substrate	9 Å^2

[a] Values for the highest resolution shell (1.94–1.90 Å) are given in parentheses. [b] Numbers in parentheses correspond to observations with $I > 2\sigma(I)$. [c] Using a randomly chosen set of 5% of the reflections.[22]

[1] J. Stubbe, W. A. van der Donk, *Chem. Rev.* **1998**, *98*, 705–762.
[2] J. Rétey, *Angew. Chem.* **1990**, *102*, 373–379; *Angew. Chem. Int. Ed. Engl.* **1990**, *29*, 355–361.
[3] *Vitamin B_{12} and B_{12}-Proteins* (Eds.: B. Kräutler, D. Arigoni, B. T. Golding), Wiley-VCH, Weinheim, **1998**.
[4] J. Halpern, *Science* **1985**, *227*, 869–875.
[5] S. Licht, G. J. Gerfen, J. Stubbe, *Science* **1996**, *271*, 477–481.
[6] B. T. Golding, R. J. Anderson, S. Ashwell, C. H. Edwards, I. Garnett, F. Kroll, W. Buckel in *Vitamin B_{12} and B_{12}-Proteins* (Eds.: B. Kräutler, D. Arigoni, B. T. Golding), Wiley-VCH, Weinheim, **1998**, pp. 201–216.
[7] F. Mancia, N. H. Keep, A. Nakagawa, P. F. Leadlay, S. McSweeney, B. Rasmussen, P. Bosecke, O. Diat, P. R. Evans, *Structure* **1996**, *4*, 339–350.
[8] F. Mancia, P. R. Evans, *Structure* **1998**, *6*, 711–720.
[9] R. Reitzer, K. Gruber, G. Jogl, U. G. Wagner, H. Bothe, W. Buckel, C. Kratky, *Structure* **1999**, *7*, 891–902.
[10] N. Shibata, J. Masuda, T. Tobimatsu, T. Toraya, K. Suto, Y. Morimoto, N. Yasuoka, *Structure* **1999**, *7*, 997–1008.
[11] H. Bothe, D. J. Darley, S. P. J. Albracht, G. J. Gerfen, B. T. Golding, W. Buckel, *Biochemistry* **1998**, *37*, 4105–4113.
[12] G. J. Gerfen in *Chemistry and Biochemistry of B_{12}* (Ed.: R. Banerjee), Wiley, New York, **1999**, pp. 165–195.
[13] G. J. Gerfen, S. Licht, J. P. Willems, B. M. Hoffman, J. Stubbe, *J. Am. Chem. Soc.* **1996**, *118*, 8192–8197.
[14] E. N. G. Marsh, D. P. Ballou, *Biochemistry* **1998**, *37*, 11864–11872.
[15] R. Padmakumar, R. Padmakumar, R. Banerjee, *Biochemistry* **1997**, *36*, 3713–3718.
[16] a) Glutamate mutase is known to lose its activity in the presence of substrate within several hours with concomitant formation of protein-bound cob(II)alamin.[16b] It is not known whether this inactivation also occurred under the crystallization conditions (see Experimental Section). In any case, there is no doubt that the two species (A and B) are structurally related to reaction intermediates b and c of Scheme 2. b) O. Zelder, B. Beatrix, U. Leutbecher, W. Buckel, *Eur. J. Biochem.* **1994**, *226*, 577–585.
[17] a) M. Levitt, A. Warshel, *J. Am. Chem. Soc.* **1978**, *100*, 2607–2613; b) K. A. Brameld, W. A. Goddard III, *J. Am. Chem. Soc.* **1999**, *121*, 985–993.
[18] F. Mancia, G. A. Smith, P. R. Evans, *Biochemistry* **1999**, *38*, 7999–8005.
[19] a) In B_{12} dependent ribonucleotide reductases, EPR data[13] yielded a distance between the cobalt center and the radical mediator of around 8 Å, in the same range as the cobalt–substrate distance in Glm. For diol dehydratase, the substrate has a different position relative to the cofactor,[10] and rotation about the glycosidic bond has been proposed for radical transport.[19b] b) J. Masuda, N. Shibata, Y. Morimoto, T. Toraya, N. Yasuoka, *Structure* **2000**, *8*, 775–788.
[20] Z. Otwinowski, W. Minor, *Methods Enzymol.* **1997**, *276*, 307–326.
[21] G. M. Sheldrick, SHELXL-97, a program for the refinement of crystal structures from diffraction data, University of Göttingen, Göttingen, **1997**.
[22] G. J. Kleywegt, A. T. Brunger, *Structure* **1996**, *4*, 897–904.
[23] P. J. Kraulis, *J. Appl. Crystallogr.* **1991**, *24*, 946–950.
[24] E. A. Merritt, D. J. Bacon, *Methods Enzymol.* **1997**, *277*, 505–524.

"Carving on the Nanoscale": Polymers for the Site-Specific Dissolution of Calcium Phosphate**

Anna Peytcheva and Markus Antonietti*

In biologically mineralized systems the constructive interaction of the inorganic crystal phase with the organic matrix material results in composite materials that are exceptional in their outward appearance and material properties.[1, 2] Of the 60 minerals known to be "processed" by living organisms, the most frequently used are calcium carbonate, calcium phosphate, and hydrous silica. They are used for the formation of scales, prickles, shells, or endoskeletons. The mineral is usually crystallized within a protein or polysaccharide matrix which has a number of functions: it shapes and aligns the single-crystalline building blocks, and it serves as a ductile component for mechanical stress dissipation.[3, 4] The resulting nanoscale composite structures make biominerals such as bone or teeth superior to most artificial ceramics.

One of the reoccurring motives in biomineralization is that the polymer controls the crystal structure or the biomineral shape, in that the crystal surface is stabilized by an opposite, complementary form of the polymer, which results in an overall structure of minimal energy.[5, 6] This method can be described by ideas that originate from solid-state physics ("finding epitaxial relations"), but that do not consider polymer flexibility or adaptability. For simplicity, this class of models is called "energetical" models.

On the other hand, it is well known in biomedicine and colloid chemistry that crystals in equilibrium with a supporting aqueous phase are not static objects but are continuously reconstructed. Thus the crystal shape is the result of dynamic processes, that is, the crystal geometries which are built up fastest and dissolved slowest are those that survive. A model based upon interfacial energies and kinetics was introduced and improved over the years by Nancollas and Wu[7] with a special emphasis on calcium phosphates. Here, the influence of a polymer or the biomatrix is purely kinetic, the structure-controlling molecules are not necessarily bound to the surface, but act by lowering the averaged surface energy, and an epitaxial fit of polymer and crystal is not required. We call this mode of operation the "kinetic" mode.

Although important for biomedicine and for controlled nanoparticle synthesis, there is still some controversy about the validity of both mechanisms. The development of scanning force microscopy (SFM) allowed the visualization of dissolution and growth processes in water in a time-resolved fashion.[8, 9] First experiments focused on the influence of low molecular weight components such as aspartic acid[10] or magnesium ions[11] on the growth of calcium carbonate. Also

---

[*] Prof. Dr. M. Antonietti, Dr. A. Peytcheva
Max Planck Institute of Colloids and Interfaces
Am Mühlenberg 1, 14476 Golm (Germany)
Fax: (+49) 331-567-9502
E-mail: pape@mpikg-golm.mpg.de

[**] Financial support by the Max Planck Society is gratefully acknowledged We thank Dr. H. Cölfen, MPI Golm and Dr. H. Schnablegger, Universität Hamburg, for helpful discussions..